

# High Performance Dense Wavelength Division Multiplexer Based on Blazed Grating and Ion-exchanged Glass Waveguide Technique

Jizuo Zou<sup>\*</sup>, Feng Zhao, Ray T. Chen

Microelectronics Research Center, J.J. Pickle Research Campus  
The University of Texas at Austin  
10100 Burnet Road, Austin, TX 78758

## ABSTRACT

Data bit rate, 1dB pass band and device dimensions are the key properties of dense wavelength division multiplexer (DWDM) devices. For blazed grating based DWDM structure, analysis shows that the bit rate is limited by the pulse broadening introduced by the grating. To reduce the pulse broadening, the output fiber array channel-to-channel pitch must be reduced. By decreasing the output channel pitch, 1dB pass band can be increased and the device dimensions can be shrunk. In this paper, we propose an ion-exchanged glass waveguide chip to be inserted into the WDM device in order to reduce the output channel spacing. To fabricate the low loss fiber compatible waveguides, two-step  $K^+-Na^+$  and  $Ag^+-Na^+$  ion-exchange process using BK7 glass as the substrate has been investigated. The optimal process conditions have been found. The waveguides fabricated by this two-step process have a propagation loss of 0.3dB/cm, a coupling loss to single mode fiber of 0.4dB and a polarization dependent loss of 0.1dB for 5cm long waveguides. The design of a 48 channel DWDM with this glass waveguide chip is given.

**Key words:** DWDM, Pulse Broadening, Ion-exchange, Glass Waveguide

## 1. INTRODUCTION

Various technologies have been applied to carry out the wavelength division multiplexing/demultiplexing (WDM/WDDM). Currently, four major categories are widely used: thin film filters (TFF), arrayed waveguide gratings (AWG), fiber Bragg gratings (FBG)<sup>[1]</sup>, and free-space diffraction grating based WDM<sup>[2]</sup>. These technologies find their applications in different situations based on their relative technical complexity, cost, performance, reliability, production yield, etc. Due to their cascade problems, TFF and FBG WDM devices are mainly attractive to the coarse WDM systems in which the channel counts are not large. For the dense WDM (DWDM) in long haul fiber communication systems, the channel count is usually higher than 40, AWG and free-space grating based WDM are the two promising candidates. The major advantages of AWG technique include its low chromatic dispersion and high integration density. However, manufacturing AWGs involves a series of complex production processes and requires bulky facilities. In addition, for AWG devices, both the temperature dependent performances and the stress-induced birefringence are big bottlenecks that are difficult to overcome. On the other hand, free-space grating based WDMs have such features as low loss, low crosstalk, low polarization dependent loss (PDL) and low temperature dependence.

In this paper, we first analyze three major challenges in free-space blazed grating based DWDMs: pulse broadening, 1dB pass band and device packaging density. Based on these analyses, we introduce an ion-exchanged single mode fiber (SMF) compatible glass waveguide chip to solve these problems. With this waveguide chip, all these challenges can be improved significantly. To fabricate the waveguide chip, we investigated a two-step  $K^+-Na^+$  and  $Ag^+-Na^+$  ion-exchange

---

<sup>\*</sup> jzou@ece.utexas.edu

process and have found the optimal fabrication conditions. The design of a 48 channel DWDM based on such a glass waveguide chip is given at the end of this paper.

## 2. CHALLENGES IN BLAZED GRATING BASED DWDMs

### 2.1 Pulse broadening

The schematic of a blazed grating based WD(D)M with a Littrow structure is shown in Fig.1, where G is the blazed grating with a blazing angle of  $\theta$ , L is the collimating and focusing lens. Here, we assume the central channel of the fiber array is the input, and the others are the outputs. The whole system works as a WDDM unit. The input light that contains various wavelengths is collimated by lens L. When the collimated light hits on the grating, the diffracted light beam of each wavelength will propagate in a specific direction. After lens L, each of these beams is focused onto a specific fiber of the fiber array and then all the wavelengths are separated into different output channels. If we inverse the input and the outputs, then the device functions as a WDM unit that combines various input wavelengths into one output channel. In the Littrow structure, the input and the output channels can be combined into one single fiber array, and lens L works as both the collimating lens and the focusing lens. The simplicity of this structure gives its great advantages over other WDM technologies.

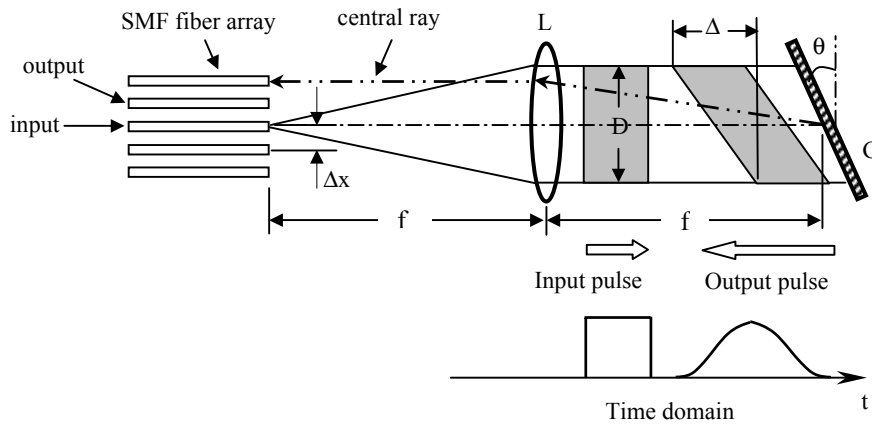


Fig. 1 Schematic of blazed grating based WD(D)M with Littrow structure

In optical communication systems, the signal carriers are laser pulses. These pulses will be broadened when they go through a WD(D)M device and therefore the data transmission bit rate will be limited. As shown in Fig.1, when the input light pulses are collimated by lens L, their wavefronts are perpendicular to the optical axis (assume the light is plane wave). However, after diffraction from grating G, the wavefronts are tilted. This wavefront tilting causes a broadening of the pulses. From Fig.1, we can see that, the lower part of the light beam is delayed compared to the upper part. Once the optical pulses are coupled into the fiber array and eventually converted into electronic signals, the electronic pulses are broadened in the time domain.

The diffraction geometry of a blazed grating is shown in Fig.2. The calculation of the pulse broadening can be done as following.

Assume: fiber-to-fiber spacing of the fiber array =  $\Delta x$ ,  
wavelength channel-to-channel spacing =  $\Delta \lambda$ ,  
focus length of lens L = f,  
diameter of the collimated beam = D,  
numerical aperture of the fibers = NA,

incident angle to the grating  $\theta_1$ ,  
diffraction angle  $\theta_2$ ,  
grating period = d,  
diffraction order = m,  
maximum optical path difference induced =  $\Delta$ .

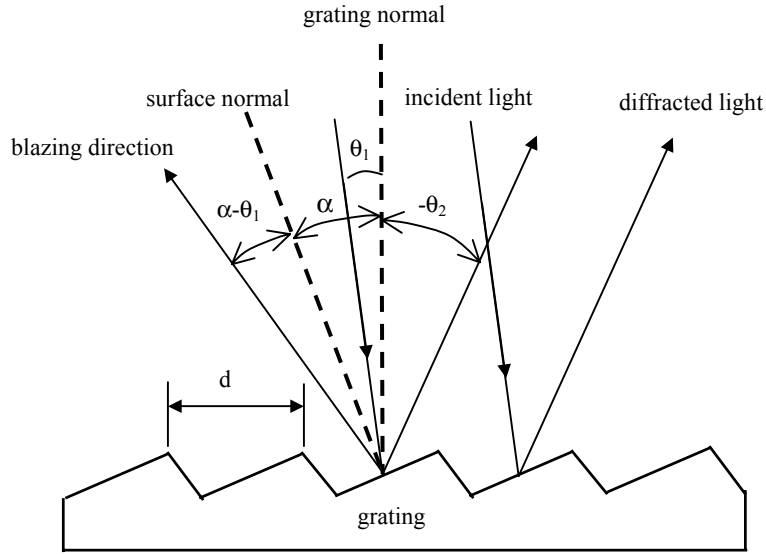


Fig. 2 Diffraction geometry of blazed grating

For Littrow structure, the incident angle and the diffraction angle are equal for the central channel. Since the displacements of the other channels are small from the central channel, the deviations of their pulse broadenings are also small. Therefore, we only calculate the broadening of the central channel for which  $\theta_1 = \theta_2 = \theta$ . Then,

$$\Delta = 2D \tan \theta \approx 4(NA)f \tan \theta . \quad (1)$$

The diffraction equation is

$$d(\sin \theta_1 + \sin \theta_2) = 2d \sin \theta = m\lambda , \quad (2)$$

where we obtain the angular dispersion,

$$\frac{d\theta_2}{d\lambda} = \frac{m}{d \cos \theta_2} = \frac{2d \sin \theta}{d\lambda \cos \theta} = \frac{2 \sin \theta}{\lambda \cos \theta} = \frac{2}{\lambda} \tan \theta . \quad (3)$$

Also,

$$\Delta x \approx f \frac{d\theta_2}{d\lambda} \Delta \lambda = \Delta \lambda \frac{2}{\lambda} f \tan \theta , \quad (4)$$

then,

$$f \tan \theta \approx \frac{\lambda \Delta x}{2\Delta \lambda} . \quad (5)$$

Finally,

$$\Delta \approx 4(NA) \frac{\lambda \Delta x}{2\Delta \lambda} = 2(NA)\lambda \frac{\Delta x}{\Delta \lambda} \quad (6)$$

From Eq. (6), for a Littrow setup, the maximum optical path difference induced by the grating depends on the numerical aperture NA, the wavelength  $\lambda$  and the ratio  $\Delta x/\Delta\lambda$ . To reduce  $\Delta$ , we can decrease the numerical aperture NA, and/or the ratio  $\Delta x/\Delta\lambda$ . Standard SMF has a NA value of about 0.14. The ratio  $\Delta x/\Delta\lambda$  of a dense WDM(DWDM) is much larger than a coarse WDM(CWDM), which means that in DWDMs the pulse broadening problem is more serious.

The seriousness of this broadening problem can be shown quantitatively by adopting typical parameter values. For example, if  $NA=0.14$ ,  $\lambda=1550nm$ ,  $\Delta x=127\mu m$ ,  $\Delta\lambda=0.8nm$ , then the maximum delay in the spatial domain is about 68.9mm, which corresponds to a broadening of 0.23ns in the time domain.

## 2.2 1dB pass band

1dB pass band is another key parameter of a WDM device. It is the wavelength shift when the output power drops 1dB from the peak (usually at the nominal wavelength of the channel). This parameter is the indicator of the wavelength tolerance of the light source. When both the light intensity and the single mode fiber mode profile are Gaussian, the output power spectrum will also be a Gaussian shape. The definition of 1dB pass band is shown in Fig.3.

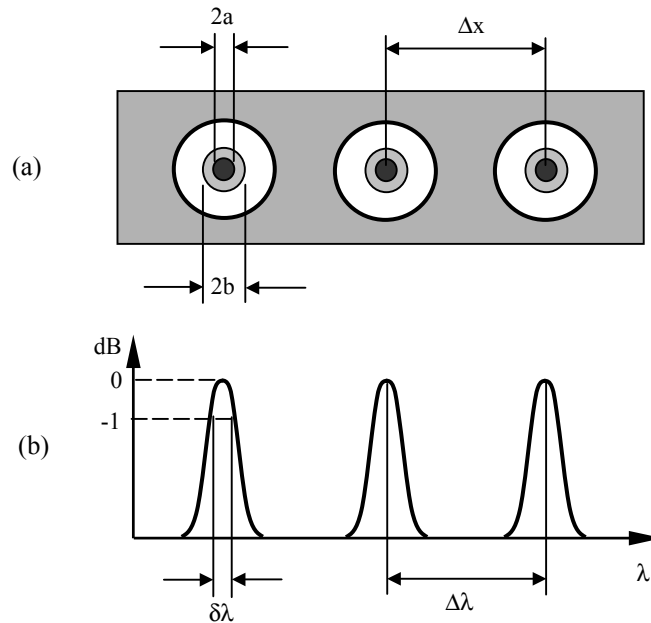


Fig. 3 Definition of 1dB pass band (a) fiber array cross section (b) output spectrum

Assume the mode field diameter of the SMF and the output image after lens L are  $2a$  and  $2b$  respectively, and Lens L is diffraction limited, then,

$$2b = \sqrt{(2a)^2 + \left(\frac{1.22\lambda}{NA}\right)^2}. \quad (7)$$

The second term on the right hand side of Eq.(7) is caused by the diffraction due to the limited beam size. Here, we use the full width at  $1/e^2$  of the intensity maximum as the definition of the field diameter. The output spectrum can be calculated by convoluting the output image with the SMF profile. The 1dB pass band is,

$$\delta\lambda = 0.68\sqrt{2a^2 + \left(\frac{0.61\lambda}{NA}\right)^2} \left(\frac{\Delta\lambda}{\Delta x}\right). \quad (8)$$

Clearly, 1dB pass band is proportional to the ratio  $\Delta\lambda/\Delta x$ . To have larger 1dB pass band, the output fiber-to-fiber spacing  $\Delta x$  should be as small as possible.

### 2.3 Device dimensions

The device size is a key property for integrated optical components. To compete with other technologies, both the design and the fabrication should be optimized to reduce the whole device size as much as possible. For the blazed grating based WD(D)M devices, one design rule is the tele-centric arrangement of the optics. As shown in Fig. 1 again, both the end face of the fiber array and the center of the grating are on the focus planes of lens L. With the tele-centric arrangement, the central ray of each output light cone is always normal to the endface of the fiber array so that the best coupling efficiency to the fiber can be obtained. Thence, the distance from the fiber array to the grating center is twice the focus length of lens L if the lens thickness is neglected. On the other hand, the beam diameter of the collimated light is also proportional to the focus length. By reducing the focus length of lens L, both the lens diameter and the grating effective area can be reduced, which results in three-dimensional shrinkage of the whole device size.

The required focus lens is

$$f = \left(\frac{\Delta x}{\Delta\lambda}\right) / \left(\frac{d\theta_2}{d\lambda}\right) \quad (9)$$

The second term on the right hand side of Eq.(9) is the angular dispersion of the grating. Once the grating is selected, the value of this term will be fixed. Therefore, the focus length  $f$  is proportional to the ratio  $\Delta x/\Delta\lambda$ . To reduce the focus length, the output fiber-to-fiber spacing should be decreased.

## 3. HIGH PERFORMANCE DWDM WITH GLASS WAVEGUIDE TECHNIQUE

### 3.1 Approach to the challenges: ion-exchanged glass waveguide

From the above analyses, the three challenges in a grating based DWDM device all rely on one parameter, the output fiber-to-fiber spacing. By reducing this spacing value, the pulse broadening and the device dimensions can be reduced proportionally, and the 1dB pass band can be increased. Standard SMF fiber array has a pitch size of  $250\mu\text{m}$  or  $127\mu\text{m}$ . To effectively reduce the pitch size, our approach is to attach a piece of ion-exchanged glass waveguide concentrator chip before the standard fiber array. The waveguide channel spacing is designed to be about  $18\mu\text{m}$  at the end that collects the diffracted output light and  $127\mu\text{m}$  at the other end that connects to the standard fiber array. The schematic drawing of such a DWDM is shown in Fig. 4.

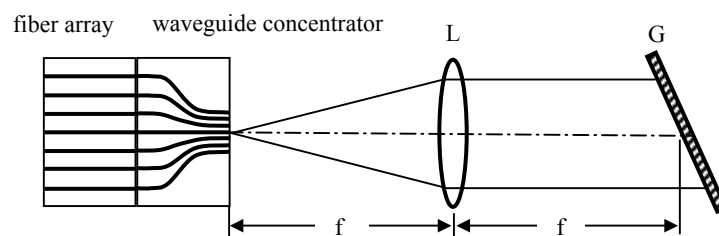


Fig. 4 Blazed grating based DWDM with ion-exchanged glass waveguide concentrator

Ion-exchanged glass waveguide has a lot of advantages. First, the refractive index of glass can be very close to that of the fibers, then the reflection at the interface between the waveguides and the fibers could be very low. Second, by carefully choosing the glass type, the absorption at C-band could be very low. Third, most glasses have no birefringence. Finally and mostly attractively, ion-exchange process is very simple and does not require expensive facilities. For the waveguide concentrator chip used in the DWDM device shown in Fig. 4, the crucial properties include propagation loss, coupling loss to SMF, polarization dependent loss (PDL), minimum bending curvature and crosstalk between adjacent channels. In the following session, a two-step  $K^+$ - $Na^+$  and  $Ag^+$ - $Na^+$  ion-exchange process will be introduced to fabricate the waveguide chip. After that, the design of the DWDM will be discussed.

### 3.2 Two-step $K^+$ - $Na^+$ and $Ag^+$ - $Na^+$ ion-exchange process

Ion-exchange has been considered as one of the most successful waveguide fabrication methods in recent years and a lot of publications regarding to the mechanisms, the process details and the applications can be found<sup>[3][4]</sup>. Basically, the driving mechanism of the ion-exchange process is diffusion. Most glass materials contain sodium. At certain temperature (usually 300-500°C), the sodium ions  $Na^+$  can be interchanged by other ions such as  $K^+$ ,  $Ag^+$  or  $Tl^+$  through thermal diffusion if the glass is contacted with such sources that contain these ions. These ions cause higher refractive index of glass than  $Na^+$  does. If a metal mask is constructed on the glass surface to define channel regions that will allow the ion-exchange to occur, then optical waveguides can be formed. Commonly used ions are  $K^+$  and  $Ag^+$ , and the ion sources are  $KNO_3$  and  $AgNO_3$ . Due to the low value in the refractive index difference between  $K^+$  and  $Na^+$ ,  $K^+$ - $Na^+$  ion-exchange is mostly used for single mode waveguide fabrication. On the other hand,  $Ag^+$  causes much higher refractive index of glass than  $K^+$ , and therefore  $Ag^+$ - $Na^+$  ion-exchange is suitable for multimode waveguide fabrication. Certainly, fabrication of single mode waveguides by  $Ag^+$ - $Na^+$  process is also possible. In such a case, both the  $Na^+$  concentration in the glass material and the  $Ag^+$  concentration in the ion source should be kept low enough. The ion-exchange process could be pure thermal or electric field assisted. By applying electric field, the guided region can be buried below the glass surface to confine more circular mode profiles and reduce the surface scattering losses. However, the field-assisted process is more complicated than the pure thermal process. In this paper, we introduce a two-step  $K^+$ - $Na^+$  and  $Ag^+$ - $Na^+$  ion-exchange method to fabricate semi-buried single mode glass waveguides. Detailed investigation of this process has been published elsewhere<sup>[5]</sup>, only the basic idea and the results will be given here.

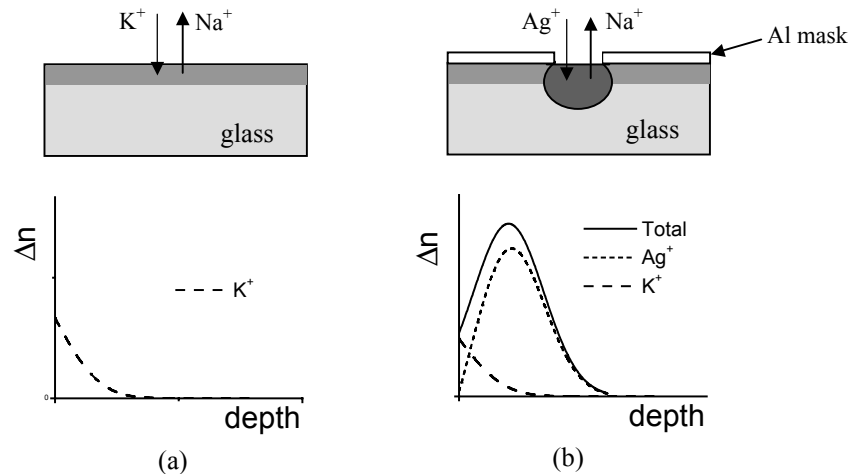


Fig. 5 Two-step  $K^+$ - $Na^+$  and  $Ag^+$ - $Na^+$  ion-exchange concept  
(a) first step  $K^+$ - $Na^+$  (b) second step  $Ag^+$ - $Na^+$

We selected BK7 as the glass substrate for the waveguide fabrication. BK7 is a good candidate material for single mode waveguide fabrication owing to its low sodium concentration, high transmittance at telecom wavelength region and low cost. The two-step  $K^+$ - $Na^+$  and  $Ag^+$ - $Na^+$  ion-exchange concept is shown in Fig. 5. During the  $K^+$ - $Na^+$  step,  $K^+$  ions enter

the thin surface layer of the glass wafer and a refractive index profile of a complementary error function along the depth direction is obtained. The diffusion time and the diffusion temperature are chosen appropriately so that this layer is thin enough not to support any waveguide modes. During the  $\text{Ag}^+\text{-Na}^+$  step, the  $\text{Ag}^+$  ions can diffuse through the  $\text{K}^+$  layer since the first step ion-exchange is not complete and there is a small percentage of  $\text{Na}^+$  left. Usually the diffusion temperature in the second step is much lower than that in the first step, so the  $\text{K}^+$  layer does not change during the second step. Since the  $\text{Ag}^+$  ions cause much higher refractive index increase than the  $\text{K}^+$  ions, the peak of the total refractive index profile is actually below the glass surface, and therefore buried waveguides are obtained.

The two-step process has a few advantages compared to the one-step  $\text{Ag}^+\text{-Na}^+$  process. With the  $\text{K}^+$  layer, the gradient of the  $\text{Na}^+$  concentration in the glass surface layer will be larger in the depth direction than in the lateral direction. Thus, during the second step ion-exchange, the diffusion speed of  $\text{Ag}^+$  ions will be faster in the depth direction than in the lateral direction. This will result in less side diffusion, which gives more circular mode profile. At the same time, less side diffusion necessitates wider mask openings for SMF-compatible waveguide fabrication. Certainly, the burying of the waveguides reduces the scattering loss and the absorption loss induced by the colloidal silver particles formed under the edges of the Al mask<sup>[6]</sup>. Compared to the field assisted process, this two-step method is simpler, no special procedures and facilities are required.

To further reduce the propagation loss caused by the precipitation of the metallic silver particles, diluted  $\text{AgNO}_3$  melt ( $\text{AgNO}_3\text{:NaNO}_3=0.1\text{:}1$  mole) is used. In addition, after the second step ion-exchange, the waveguides are annealed at  $300^\circ\text{C}$  for 12 to 24 hours. By annealing, metallic silver atoms can diffuse into the glass and change into silver ions and in the mean time, the mode profile can be enlarged to match better with SMF.

With two-step  $\text{K}^+\text{-Na}^+$  and  $\text{Ag}^+\text{-Na}^+$  ion-exchange, we have obtained propagation loss of  $0.3\text{dB/cm}$ , coupling loss to/from SMF of  $0.4\text{dB}$  and PDL of less than  $0.1\text{dB}$  for  $5\text{cm}$  long waveguides. The best channel width is around  $9\text{-}10\mu\text{m}$ , and the best bending structure for the waveguide concentrator is cosine curve. For the concentrator structure, the maximum crosstalk between two adjacent channel is lower than  $-30\text{dB}$ .

### 3.3 DWDM design

Nowadays, both the channel numbers and the bit rate of each channel in WDM systems are increasing. However, due to the limited wavelength window and the transmission bandwidth of optical fibers, there must be a trade off between these two parameters. Up to now, based on the availabilities of WDM lasers, modulators and detectors,  $40\text{Gb/s}$  per channel is possible and actually has been demonstrated with AWG devices. To efficiently use the transmission bandwidth, for a  $40\text{Gb/s}$  bit rate of a single channel, the minimum channel spacing should be around  $100\text{GHz}$ . Therefore, in our grating based DWDM device, the channel spacing is set to  $100\text{GHz}$  corresponding to the ITU grid. The channel number is 48 to cover the whole C-band centered at wavelength of  $1550\text{nm}$ .

To minimize the PDL of our DWDM device, the blazed grating should have minimum dependence on the polarization of the incoming light. A  $600\text{g/mm}$  grating with the same 1<sup>st</sup> order diffraction efficiency for both p-wave and s-wave at  $1550\text{nm}$  is selected in our device. Within the whole C-band window, the diffraction efficiency difference between these two polarizations is within several percent. The substrate material of the grating has very low thermal expansion coefficient.

To minimize the coupling loss to the output waveguides, the collimating lens should have best imaging quality, which requires a diffraction-limited design. For a DWDM device, even the wavelength range is only  $40\text{nm}$  for C-band coverage the chromatic aberration is still a serious problem. The lens materials have been carefully chosen to minimize this aberration.

Based on our waveguide fabrication technique, the waveguide concentrator is designed to have a channel spacing non linearly spaced from  $18\mu\text{m}$  to  $19\mu\text{m}$  at one end and have a standard spacing of  $127\mu\text{m}$  at the other end. The waveguide pattern has a cosine curve with a channel width of  $9\mu\text{m}$ .

Packing design of the DWDM device is a challenging work. To minimize the sensitivity of the device performances to the ambient temperature change, different materials can be used for the lens holder, the base plate and the waveguide holder to compensate their thermal coefficients. In the meantime, the whole device is designed as epoxy free. With the technical performances satisfied, the packaging density should be always kept as high as possible.

Based on the design criteria given above, the 48 channel DWDM with ion-exchanged glass waveguide technique is proposed to have maximum pulse broadening of 0.03ns, 1dB pass band of 0.3nm, and insertion loss of -5dB.

#### 4. CONCLUSIONS

In this paper, the major challenges in blazed grating based DWDM devices are discussed. From the analyses we found that all of these challenges directly rely on the minimizing of the output fiber-to-fiber spacing of the fiber array. To effectively reduce this spacing, a glass waveguide concentrator fabricated by ion-exchange process is attached to the standard fiber array. With this waveguide concentrator, all these challenges of the DWDM device can be improved significantly. To fabricate the waveguide chip, a two-step  $K^+Na^+$  and  $Ag^+Na^+$  ion-exchange process was investigated and optimal fabrication conditions have been found. The waveguide made by this process has shown a propagation loss of 0.3dB/cm, a coupling loss to/from SMF of 0.4dB and very low PDL. Based on the waveguide chip and the Littrow structure, the device design criteria are also discussed.

#### REFERENCES

1. Yoshinori Hibino, "Passive optical devices for photonic networks", IEICE Trans. Commun., Vol.E83-B, No.10, p2178-2190 (2000)
2. Feng Zhao, et al, "Wavelength division multiplexers/demultiplexers for high-throughput optical links", Proc. SPIE, Vol. 4653, p172-181(2002).
3. R.V. Ramaswamy and R. Srivastava, "Ion-exchanged glass waveguides: a review", J. Lightwave Technol., Vol.6, No.6, p984-1002 (1988).
4. S. Iraj Najafi, "Introduction to Glass Integrated Optics" (Artech House, Boston, 1992).
5. Jizuo Zou, Feng Zhao and Ray T. Chen, "Two-step  $K^+Na^+$  and  $Ag^+Na^+$  ion-exchanged glass waveguides for C-band applications", Appl. Opt., Vol.41, No.36, p7620-7626 (2002).
6. R.G. Walker and C.D.W. Wilkinson, "Integrated optical waveguiding structures made by silver ion-exchange in glass. 2: Directional coupler and bends," Appl. Opt., Vol.22, No.12, p1929-1936 (1983).